Reaction of atomic hydrogen with formic acid

Cao, Qian

2014

Cao , Q , Berski , S , Latajka , Z , Räsänen , M & Khriachtchev , L 2014 , ' Reaction of atomic hydrogen with formic acid ' , Physical Chemistry Chemical Physics , vol. 16 , no. 13 , pp. 5993-6001 . https://doi.org/10.1039/c3cp55265a

http://hdl.handle.net/10138/224678
https://doi.org/10.1039/c3cp55265a

PCCP

PAPER

View Article Online
View Journal | View Issue

Reaction of atomic hydrogen with formic acid†

Cite this: *Phys. Chem. Chem. Phys.*, 2014, **16**, 5993

Qian Cao,[a] Slawomir Berski,[b] Zdzislaw Latajka,[b] Markku Räsänen[a] and Leonid Khriachtchev*[a]

Received 13th December 2013,
Accepted 29th January 2014

DOI: 10.1039/c3cp55265a

www.rsc.org/pccp

We study the reaction of atomic hydrogen with formic acid and characterize the radical products using IR spectroscopy in a Kr matrix and quantum chemical calculations. The reaction first leads to the formation of an intermediate radical *trans*-H_2COOH, which converts to the more stable radical *trans–cis*-$HC(OH)_2$ *via* hydrogen atom tunneling on a timescale of hours at 4.3 K. These open-shell species are observed for the first time as well as a reaction between atomic hydrogen and formic acid. The structural assignment is aided by extensive deuteration experiments and *ab initio* calculations at the UMP2 and UCCSD(T) levels of theory. The simplest geminal diol radical *trans–cis*-$HC(OH)_2$ identified in the present work as the final product of the reaction should be very reactive, and further reaction channels are of particular interest. These reactions and species may constitute new channels for the initiation and propagation of more complex organic species in the interstellar clouds.

Introduction

Reactions of atomic hydrogen with various molecules are fundamental in combustion, atmospheric, and interstellar chemistry as well as in biology. These reactions can occur with a variety of inorganic and organic species.[1–7] Reactions of atomic hydrogen with organic compounds, especially with hydrocarbons, have been extensively studied;[1–3] however, relatively little information is available on reactions with organic acids. A very early report on the hydrogen abstraction reaction in acetic acid ($H + CH_3COOH \rightarrow CH_2COOH + H_2$) in aqueous solution seems to be the only experimental example of a reaction between an organic acid and atomic hydrogen.[8]

Formic acid (FA) is the simplest organic acid that is an important intermediate in chemical synthesis and significant in atmospheric and interstellar chemistry as well as in human metabolism. Reactions of FA with OH and Cl radicals have been studied, which are important sources of the hydrocarboxyl radical (HOCO) in the atmosphere.[9] The reaction of Cl with FA was found to proceed predominantly *via* abstraction of the hydrogen atom from the carbon atom to form HOCO rather than the abstraction of the hydroxyl hydrogen to form HCO_2.[10,11] FA is a model system of conformational isomerism resulting from different orientations of the OH group (*trans* and *cis*),[12] which is typical for carboxylic acids, including amino acids. Conformational changes promoted by vibrational excitation and the back-reaction *via* hydrogen atom tunneling have been reported for different carboxylic acids, such as FA, acetic acid, and propionic acid.[12–14] Hydrogen atom tunneling has also been recently reported for the simplest aromatic carboxylic acid, benzoic acid.[15] The conformation-dependent reaction between FA and atomic oxygen was observed in Kr and Xe matrices.[16] The FA + O reaction leads to peroxyformic acid (HCOOOH) for the ground-state *trans*-FA conformer, and it results in the hydrogen bonded FA···O complex for the higher-energy *cis*-FA conformer.[16] To the best of our knowledge, no direct experimental and theoretical data are available for the reaction of FA with atomic hydrogen to date. It should be emphasized that the present work investigates the reaction of a *neutral* hydrogen atom with FA forming radicals. This reaction is different from FA protonation, which is a known process leading to closed-shell species.

Reactions of atomic hydrogen with organic compounds can produce radicals; for example, the hydrogen atom abstraction and molecular hydrogen formation are observed for ethane whereas the hydrogen atom addition to the unsaturated carbon atom occurs for ethylene resulting in the formation of a vibrationally excited C_2H_5 radical.[1,2] Hydrogen atom transfer plays a significant role in many organic and biological reactions. In particular, the radical isomerization *via* intramolecular hydrogen atom transfer in species with the C–H, O–H, and C=O bonds often occurs in peptide and protein radicals as a result of radiation or oxidative damage.[17,18]

[a] *Department of Chemistry, University of Helsinki, P.O. Box 55, FI-00014 Helsinki, Finland. E-mail: leonid.khriachtchev@helsinki.fi; Tel: +358 919150310*
[b] *Faculty of Chemistry, University of Wroclaw, 14, F. Joliot-Curie Str., 50-383 Wroclaw, Poland*

† Electronic supplementary information (ESI) available: The optimized geometries of the species under consideration at the UPM2 and UCCSD(T) levels of theory (Table S1), the calculated vibrational frequencies and intensities of *trans*-H_2COOH, *trans–cis*-$HC(OH)_2$ and their deuterated analogues at the UPM2 level of theory (Table S2), and the total energy for hydrogen atom transfer from *trans*-H_2COOH to *trans–cis*-$HC(OH)_2$ along the IRC path (Fig. S1). See DOI: 10.1039/c3cp55265a

It is probable that reaction of atomic hydrogen with FA produces radicals *via* hydrogen atom addition, which may then isomerize *via* intramolecular hydrogen transfer.

Matrix-isolation IR spectroscopy is a valuable method to study reactive intermediates obtained in reactions of atomic hydrogen. In our group, the H + C_2H_2 → C_2H_3,[19] H + HCN → H_2CN,[20] H + HNCO → H_2NCO,[21] and H + N_2O → HN_2O[22] reactions have been detected in rare-gas matrices, in which the hydrogen atoms are produced by photolysis of suitable precursors (*e.g.*, C_2H_2, HCN, HNCO, and HBr) and the formed radicals are characterized by IR spectroscopy. An interesting case is the H + SO_2 reaction.[23] The higher-energy HSO_2 isomer is formed in this reaction instead of the lower-energy isomer *cis*-HOSO, which is explained by a low barrier for the HSO_2 formation and a high barrier for the *cis*-HOSO formation. HSO_2 can be isomerised into *cis*-HOSO by visible light, one proposed mechanism of which is the direct isomerisation *via* intramolecular hydrogen atom transfer.

In the present work, we study the reactions of hydrogen atoms with FA in a Kr matrix and characterize the radical products using IR spectroscopy. Hydrogen (deuterium) atoms are produced by UV photolysis of HBr and HCl (D_2C_2). Thermal mobilization of the hydrogen atoms promotes the H + FA reaction, leading first to the formation of an intermediate radical *trans*-H_2COOH, which converts *via* hydrogen atom tunneling to the more stable radical *trans–cis*-$HC(OH)_2$. The structural assignment is aided by extensive deuteration experiments and *ab initio* calculations at the UMP2 and UCCSD(T) levels of theory.

Computational details and results

The optimization of the geometrical structures and calculation of the relative energies and vibrational spectra were performed using the UCCSD(T) and UMP2 methods with the aug-cc-pVTZ basis set. The Molpro program was used for the UCCSD(T) calculations and Gaussian09 (version C.01) for the UMP2 calculations. The minima on the potential energy surface (PES) were verified on the basis of harmonic vibration analysis which yielded no imaginary frequencies. In the case of the transition state (TS), one imaginary frequency was obtained. The minima on the PES associated with the TS were verified by means of the intrinsic reaction coordinate (IRC) analysis. The relative energy (ΔE) between the optimized geometrical structures was corrected for the zero-point vibrational energy difference (ΔZPVE).

The reaction of a hydrogen atom with FA may proceed by three different channels: (i) reaction with the oxygen atom of the hydroxyl group (OH), (ii) reaction with the oxygen atom of the carbonyl group (C═O), and (iii) reaction with the carbon atom. These channels have been studied by the UMP2/aug-cc-pVTZ and UCCSD(T)/aug-cc-pVTZ calculations. For channel (i), no minimum was found on the PES. This process results in the formation of a new H–O bond, the breaking of the C–O bond and the formation of a water molecule, which finally leads to the HCO···H_2O complex. Two other channels produce radicals shown in Fig. 1. For channel (ii), the $HC(OH)_2$ radical is formed that accepts two conformers. The two O–H bonds can be oriented in the same direction as the C–H bond (*cis–cis* form) or one O–H bond can be oriented in the opposite direction to the C–H bond (*trans–cis* form). These structures present the simplest geminal diol radicals. The *trans–trans* form of $HC(OH)_2$ is a transition state with one imaginary frequency, which is above the *trans–cis* form by about 1.55 kcal mol^{-1} (UMP2). Channel (iii) leads to the H_2COOH radical with two C–H bonds and one O–H bond which may be oriented in two directions as shown in Fig. 1. The *trans* conformer has an out-of-plane OH bond (∠O–C–O–H = 56°) and two non-equivalent CH bonds. The analysis shows that the *cis* form has practically no stabilization barrier; thus, it can be excluded from the consideration. The optimized geometries of the species under consideration are presented in Table S1, ESI.†

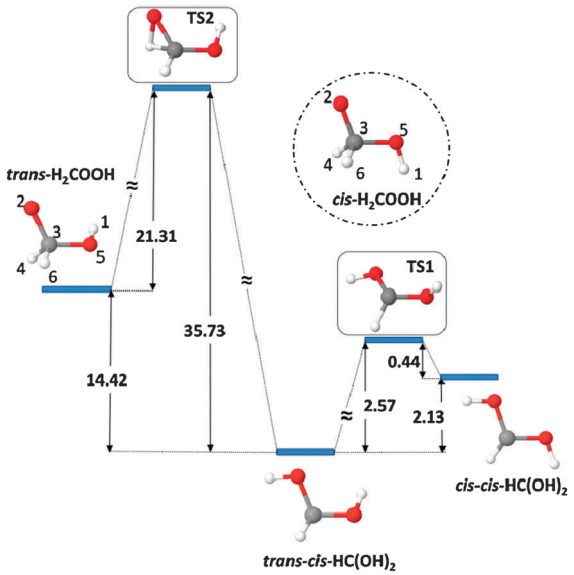

Fig. 1 Schematic potential energy diagram of the radicals that may be formed in the H + HCOOH reaction. The energy values (in kcal mol^{-1}) are calculated at the UMP2 level (for the UCCSD(T) energies of the optimized structures see Table 1). The structures shown in rectangles are transition states (TS1 and TS2); *cis*-H_2COOH (shown in a dashed circle) is energetically unfavourable. In *trans*-H_2COOH, H1 and H4 are on the same side of the heavy-atom skeleton.

The energetic effect associated with the formation of the new bonds, H–O in $HC(OH)_2$ and H–C in H_2COOH, is characterized by the reaction energy (ΔE_r) calculated for the reactions:

$$H + HCOOH \rightarrow HC(OH)_2 \quad (1)$$

$$H + HCOOH \rightarrow H_2COOH \quad (2)$$

The value of ΔE_r is the difference between the total energy of the $HC(OH)_2$ or H_2COOH radical and the sum of the total energies of the hydrogen atom and FA (the lowest energy form) corrected by ΔZPVE (see Table 1). The formation of the $HC(OH)_2$ radical is energetically favourable for both UMP2

Table 1 Energetics (in kcal mol^{-1}) for the radicals that may be formed in the H + HCOOH reactions calculated at the UCCSD(T) and UMP2 (in parentheses) levels of theory

	Relative energy (ΔE + ZPVE)		Reaction energy (ΔE_r + ZPVE)	
trans–cis-HC(OH)$_2$	0	(0)	−10.01	(−10.87)
cis–cis-HC(OH)$_2$	2.16	(2.13)	−7.85	(−8.74)
trans-H$_2$COOH	8.10	(14.42)	−1.91	(+3.55)
cis-H$_2$COOH	10.19	(16.61)	+0.17	(+5.74)

and UCCSD(T) computational methods with ΔE_r of −10.87 (*trans–cis*), −8.74 (*cis–cis*) kcal mol^{-1} and −10.01 (*trans–cis*), −7.85 (*cis–cis*) kcal mol^{-1}, respectively. For the formation of H$_2$COOH, the UMP2 method gives positive ΔE_r of 3.55 (*trans*) and 5.74 (*cis*) kcal mol^{-1}. The better description of the electron correlation using the UCCSD(T) method leads to a qualitatively different result. The formation of *trans*-H$_2$COOH is energetically favourable with negative ΔE_r (−1.91 kcal mol^{-1}) whereas positive ΔE_r (0.17 kcal mol^{-1}) is predicted for the *cis* form. *trans*-H$_2$COOH is 14.42 kcal mol^{-1} (UMP2) and 8.10 kcal mol^{-1} (UCCSD(T)) above *trans–cis*-HC(OH)$_2$ on the total energy scale. *trans–cis*-HC(OH)$_2$ is lower in energy than *cis–cis*-HC(OH)$_2$ by 2.13 kcal mol^{-1} (UMP2) and 2.16 kcal mol^{-1} (UCCSD(T)), as shown in Table 1. The isomerization from *trans–cis*-HC(OH)$_2$ to *cis–cis*-HC(OH)$_2$ requires an activation energy (E_a) of 2.57 kcal mol^{-1} (UMP2), which is several times smaller than the activation energy of the *trans*-to-*cis* reaction of FA (11.7 kcal mol^{-1}). The optimized geometrical structure of the transition state (TS1) is shown in Fig. 1. The conformational change from *trans*-H$_2$COOH to *trans–cis*-HC(OH)$_2$ requires the transfer of the hydrogen atom from the carbon atom to the carbonyl oxygen. The energy barrier associated with this process (TS2, Fig. 1) is 21.31 kcal mol^{-1} (UMP2). The energy barrier of the opposite process is substantially higher and equals 35.73 kcal mol^{-1} (UMP2). The change in the total energy for hydrogen atom transfer from *trans*-H$_2$COOH to *trans–cis*-HC(OH)$_2$ along the IRC path is shown in Fig. S1 (ESI†).

The characteristic frequencies of the proposed radicals and their deuterated analogues obtained at the UCCSD(T)/aug-cc-pVTZ level of theory are presented in Table 2. The full spectra at the UMP2/aug-cc-pVTZ levels are presented in Table S2, ESI.†

Experimental details and results

Formic acid HCOOH (99%, Kebo Lab) and its deuterated analogues DCOOH (99%, Icon Isotopes) and HCOOD (95%, IT Isotop) were degassed by several freeze–pump–thaw cycles. The FA/HY/Kr (1/2/1000) (Y = Br, Cl) and FA/C_2D_2/Kr (1/2/1000) matrices (HBr, ≥99%, Aldrich; HCl, ≥99%, Linde; C_2D_2, ≥98%, Cambridge Isotope Laboratories; Kr, ≥99.999%, AGA) were deposited onto a CsI window at 20 K in a closed cycle helium cryostat (RDK 408D, Sumitomo Heavy Industries). The IR spectra were recorded in the spectral region 4000–500 cm^{-1} at 4.3 K using a Bruker VERTEX 80 FTIR spectrometer typically using 200 scans and a resolution of 0.5 cm^{-1}. The solid matrices were photolyzed at 4.3 K using an ArF excimer laser (193 nm, MSX-250, MPB) to produce H or D atoms, typically using 1500 pulses (pulse energy density ∼12 mJ cm^{-2} and pulse duration ∼10 ns). Vibrational excitation was promoted using an optical parametric oscillator (OPO Sunlite, Continuum with IR extension) providing tunable IR light with a pulse duration of ∼5 ns, linewidth of ∼0.1 cm^{-1}, and repetition rate of 10 Hz. A Burleigh WA-4500 wavemeter measured the OPO signal frequency, providing an absolute accuracy better than 1 cm^{-1} for the IR light.

The vibrational spectra of the ground-state (*trans*) conformer of HCOOH, DCOOH, and HCOOD in a Kr matrix recorded in our experiments agree well with the literature.[24,25] 193 nm photolysis (1500 pulses) of a HCOOH/HBr/Kr (1/2/1000) matrix decomposes about 85% HBr, producing H and Br atoms. About 30% FA is also decomposed producing mainly the CO···H$_2$O complex.[24]

Annealing of a photolyzed HCOOH/HBr/Kr matrix at 31 K mobilizes hydrogen atoms in a Kr matrix,[26] which leads to the formation of new absorption bands (trace 1 in Fig. 2). Annealing of the photolyzed matrices also leads to a loss of FA. Fig. 3 shows that the amount of the products after annealing increases with the corresponding loss of FA.

The new absorption bands can be separated into two products marked by $\mathbf{I}_U$ and $\mathbf{I}_S$ (labels U and S indicate unstable and stable, respectively). Immediately after annealing, product $\mathbf{I}_U$ dominates over product $\mathbf{I}_S$. The bands of product $\mathbf{I}_U$ slowly decrease in intensity in the dark whereas the bands of product $\mathbf{I}_S$ rise (trace 1 in Fig. 4). This process is accelerated by broad band IR light of the spectrometer (trace 2 in Fig. 2). In both cases, the amounts of $\mathbf{I}_U$ and $\mathbf{I}_S$ change with the same rates. The amount of $\mathbf{I}_U$ goes to zero and the amount of $\mathbf{I}_S$ tends to saturate. These facts feature the $\mathbf{I}_U$-to-$\mathbf{I}_S$ conversion. This conversion process is also accelerated by vibrational excitation of product $\mathbf{I}_U$ at 3614 cm^{-1} by the OPO (trace 3 in Fig. 2) whereas the vibrational excitation of product $\mathbf{I}_S$ (at 3636.0 and 3598.4 cm^{-1}) does not lead to the opposite process. The same two products are observed after photolysis and annealing of HCOOH/HCl/Kr matrices (trace 4 in Fig. 2).

It is noted that several bands of the products are split, which is probably due to trapping of the molecules in different matrix sites. The sub-bands of product $\mathbf{I}_U$ are bleached with different efficiencies when exposed to narrow-band IR light. For excitation at about 3614 cm^{-1}, the band at 3613.7 cm^{-1} is efficiently bleached together with the bands at 1116.0 and 962.0 cm^{-1}. In contrast, the decrease of the bands at 3615.0, 1115.1, and 964.5 cm^{-1} is much less efficient for excitation at about 3615 cm^{-1}.

The experiments with deuterated species were also performed under the same experimental conditions. Annealing of a photolyzed HCOOD/HBr/Kr matrix initially leads to product $\mathbf{II}_U$ that then converts in the dark to two products $\mathbf{II}_S$ and $\mathbf{II}_S'$ (trace 2 in Fig. 4, see discussion below). It should be noted that FA in this matrix is, due to incomplete deuteration, a mixture of HCOOD and HCOOH (70/30), which explains the formation of some amount of products $\mathbf{I}_U$ and $\mathbf{I}_S$. In trace 2, the bands of these products are subtracted. Most indicative, the new characteristic bands are observed in the OD stretching region (2690–2650 cm^{-1}), which are absent

Table 2 Experimental ($\mathbf{I_U}$–$\mathbf{III_U}$ and $\mathbf{I_S}$–$\mathbf{III_S}$) and calculated characteristic bands of *trans*-H_2COOH and *trans*–*cis*-$HC(OH)_2$ and their deuterated analogues[a]

Initial (unstable) products

	trans-H_2COOH		*trans*-H_2COOD		*trans*-HDCOOH	
Mode	Exp. $\mathbf{I_U}$	Calc.	Exp. $\mathbf{II_U}$	Calc.	Exp. $\mathbf{III_U}$	Calc.
νOH	3615.1	3815.3	—	—	3615.1	3814.4[b]
	3613.9				3613.9	3814.4[c]
νCH	2875.0	2997.0	2872.0	2995.9	2872.0	2994.0[b]
		2865.5		2863.9		2864.8[c]
νOD	—	—	2668.1	2775.7	—	—
			2666.2			
νCD	—	—	—	—	1952.0	2091.8[b]
						2193.3[c]
$\delta COH + \delta CH_2$	1345.5	1369.3	1321.5	1342.2	1262.8	1254.1[b]
	1343.5					1272.7[c]
$\delta COH + \delta CH_2$	1271.5	1308.6	1163.5	1214.7	—	1205.5[b]
	1270.0					1196.2[c]
$\nu_a CO_2$	1116.0	1113.7	1115.0	1117.5	1093.0	1114.5[b]
	1115.0		1113.5		1091.0	1124.5[c]
$\nu_s CO_2$	964.5	1002.2	901.0	920.4	880.7	890.2[b]
	962.0					899.9[c]
δCO_2	544.1	548.1	—	523.2	540.0	544.7[b]
						542.0[c]

Final (stable) products

	trans–*cis*-$HC(OH)_2$		*trans*–*cis*-HC(OD)(OH) *trans*-OD		*trans*–*cis*-HC(OH)(OD) *cis*-OD		*trans*–*cis*-$DC(OH)_2$	
Mode	Exp. $\mathbf{I_S}$	Calc.	Exp. $\mathbf{II_S}$	Calc.	Exp. $\mathbf{II_S'}$	Calc.	Exp. $\mathbf{III_S}$	Calc.
νOH	3638.5	3836.3	3638.5	3836.4	—	—	3638.5	3836.5
	3636.0		3636.0				3636.0	
νOH	3598.4	3800.6	—	—	3598.4	3800.8	3599.4	3800.6
	3595.5				3595.5		3598.2	
	3592.8				3592.8		3594.1	
νCH	2975.2	3109.5	2975.5	3110.0	2973.5	3109.6	—	—
	—	—	2658.3	2765.3	2686.1	2792.8	—	—
			2654.0		2684.1			
νCD	—	—	—	—	—	—	2189.2	2294.1
$\delta OCH + \delta COH$	1375.5	1417.6	1369.0	1403.6	1374.5	1413.5	1313.8	1354.2
	1374.0							
$[\delta COH + \delta COH]_{oph}$	1334.5	1368.3	1264.5	1295.7	1285.0	1324.8	1288.0	1329.7
	1332.5						1285.3	
	1327.9							
	1326.0							
$[\delta COH + \delta COH]_{iph}$	1186.0	1205.3	1147.5	1174.8	1172.5	1197.3	1126.0	1154.7
							1122.0	
$\nu_a CO_2$	1129.0	1155.1	1075.5	1098.0	—	1099.4	1046.2	1059.3
	1127.0							
	1124.7							
$\nu_s CO_2$	1045.7	1065.3	939.4	1008.6	—	963.7	923.0	934.4
τCH	879.0	959.6	883.6	891.3	—	870.2	724.0	775.6

[a] Calculations at the UCCSD(T) level of theory. [b] *trans*-HDCOOH with CD deuteration in position 4 (see Fig. 1). [c] *trans*-HDCOOH with CD deuteration in position 6 (see Fig. 1).

in the case of HCOOH/HBr/Kr matrices (trace 1 in Fig. 4). Additional new strong bands are observed at 1180–1140 cm^{-1} and 901 cm^{-1}.

Annealing of a photolyzed DCOOH/HBr/Kr matrix leads to product $\mathbf{III_U}$ which converts in the dark to $\mathbf{III_S}$ (trace 3 in Fig. 4). No bands appear in this case in the OD stretching region whereas the CD stretching bands are observed for both stable and unstable products (2189.2 and 1952.0 cm^{-1}, respectively). The most characteristic bands are observed at 1288/1285 cm^{-1} for $\mathbf{III_S}$ and at 1093/1091 cm^{-1} for $\mathbf{III_U}$. The same characteristic features are detected in a HCOOH/C_2D_2/Kr matrix, however, in quite small amounts presumably due to the relatively low efficiency of the C_2D_2 photolysis. The formation of DKrCCD (920 cm^{-1})[27] confirms the presence and mobility of D atoms in the matrix. In the HCOOH/C_2D_2/Kr case, the products formed in HCOOH/HBr/Kr matrices are also observed and subtracted in trace 4. The formation of these background products is explained by the presence of H atoms probably produced by photolysis of the CO···H_2O complex, which is a photodecomposition product of FA.[24] The presence of hydrogen atoms in the matrix is evidenced by the formation of HDCCD radicals (*ca.* 1220 and 795 cm^{-1}) originated from the H + DCCD reaction.[19] In the deuteration

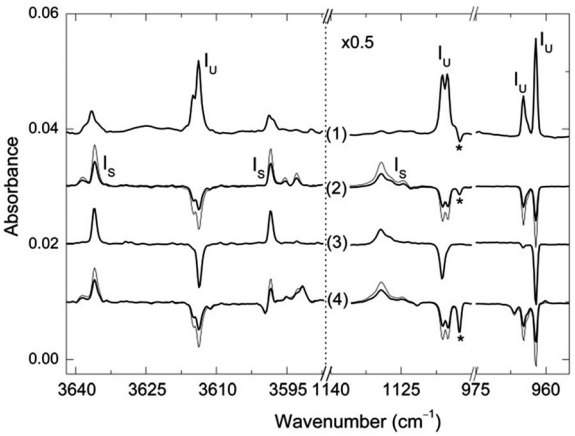

Fig. 2 Difference FTIR spectra of a HCOOH/HBr/Kr (1/2/1000) matrix photolyzed at 193 nm showing the results of (1) annealing at 31 K (5 min); (2) 1 hours (thick line) and 2 hours (thin line) at 4.3 K under Globar irradiation after annealing; (3) narrow-band IR excitation at *ca.* 3614 cm^{-1} of the annealed matrix. Trace 4 shows the difference IR spectra of a photolyzed and annealed HCOOH/HCl/Kr (1/2/1000) matrix as a result of 1 hour (thick line) and 2 hours (thin line) at 4.3 K under Globar irradiation. The spectra were recorded at 4.3 K. The bands marked by asterisks are tentatively assigned to a FA dimer (tt4).[39]

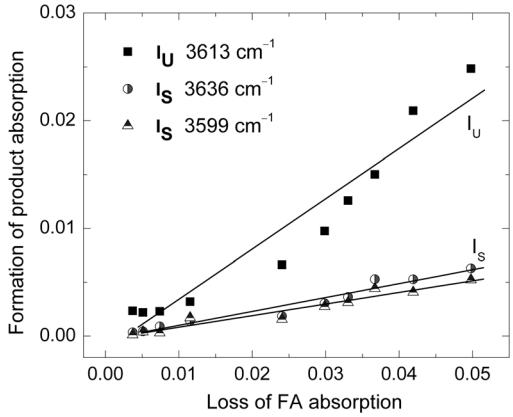

Fig. 3 Amount of products I_U and I_S *versus* the corresponding loss of FA (3536.5 cm^{-1}) in the H + FA reaction. The spectra were recorded at 4.3 K immediately after annealing at 31 K of a photolyzed HCOOH/HBr/Kr (1/2/1000) matrix. The data points correspond to the integrated intensities of the absorption bands in different experiments. The lines are linear fits.

experiments, the band intensities of the products correlate well with the annealing-induced loss of FA.

The decay of the initial products in the dark and the formation of the final products have similar rates independent of deuteration described above (characteristic time ~7.5 hours at 4.3 K, Fig. 5). The conversion is accelerated at elevated temperatures (characteristic time ~5.0 hours at 27 K). The sum of the relative intensities of the decreasing and rising bands does not change in time. The situation is absolutely different for a DCOOH/C_2D_2/Kr matrix. In this case, an annealing-induced band is observed at 3616.6 cm^{-1}, which is the OH stretching mode of the "unstable" product; however, this band does not decrease in the dark even in 45 hours. The decay of this band can be promoted by broadband light of the spectrometer. The weakness of the bands in this experiment prevents a detailed analysis in other spectral regions.

Discussion

Spectral assignments

The new products appear as a result of annealing at temperatures that mobilize hydrogen atoms in a Kr matrix.[26] It follows that the initial (unstable) product most probably originates from reactions of mobile hydrogen atoms with another fragment. For the assignment, several possibilities have been considered. First of all, the CO···H_2O complex is present in the matrix as a result of the decomposition of FA.[24] Mobile hydrogen atoms can react with this complex producing the HCO···H_2O complex, and this possibility should be discussed. In fact, the HCO···H_2O complex obtained from the H + CO···H_2O reaction has been recently identified by us,[28] and it is also observed in the present work. The formation of the HCO···H_2O complex is the most efficient when FA is mostly decomposed, *i.e.* when the amount of the CO···H_2O complex is large. As expected, the bands of the HCO···H_2O complex do not change in the dark, in contrast to the new products studied in the present work. The spectra of these products differ significantly from that of the HCO···H_2O complex. For example, the HCO···H_2O complex in a Kr matrix has a strong CO stretching band at 1853.3 cm^{-1}.[28]

The correlation between the amount of the products and the loss of FA (Fig. 3) strongly suggests that the new species originate from the H + FA reaction. The small deviation from the exact proportionality can be caused, for example, by the annealing-induced formation of FA dimers and by the consumption of hydrogen atoms in reactions with HBr. In principle, the H + FA reaction can lead to the formation of a H_2 molecule and a radical species *via* H abstraction. However, the possible radicals cannot simultaneously have the OH and CH stretching modes, which rules out this scenario.

The addition of a hydrogen atom to different positions in FA should also be considered. For example, a hydrogen atom may react with the oxygen atom of the OH group forming $HCOOH_2$. Our calculations suggest that this species is not an energy minimum, and it spontaneously decomposes to a pair of H_2O and HCO. Thus, this reaction (if occurred) would lead to the formation of the HCO···H_2O complex in a matrix.

The addition of a hydrogen atom to the oxygen atom of the C═O group is also possible, which would result in the $HC(OH)_2$ radical. The calculations show that the $HC(OH)_2$ radical has two local minima differing by the orientation of the OH groups, the higher-energy *cis–cis* form and the lower-energy *trans–cis* form (Fig. 1). Similar conformers exist for carbonic acid, although the energetics is opposite, with the *cis–cis* form being more stable than the *trans–cis* form (by 1.0–1.6 kcal mol^{-1}).[29,30] Both of these conformers of carbonic acid have been observed in an Ar matrix.[29] For this reason, we have to consider the initial formation of *cis–cis*-$HC(OH)_2$ which converts to *trans–cis*-$HC(OH)_2$. However, the calculated barrier between these two species is only 0.44 kcal mol^{-1}, which is much smaller than

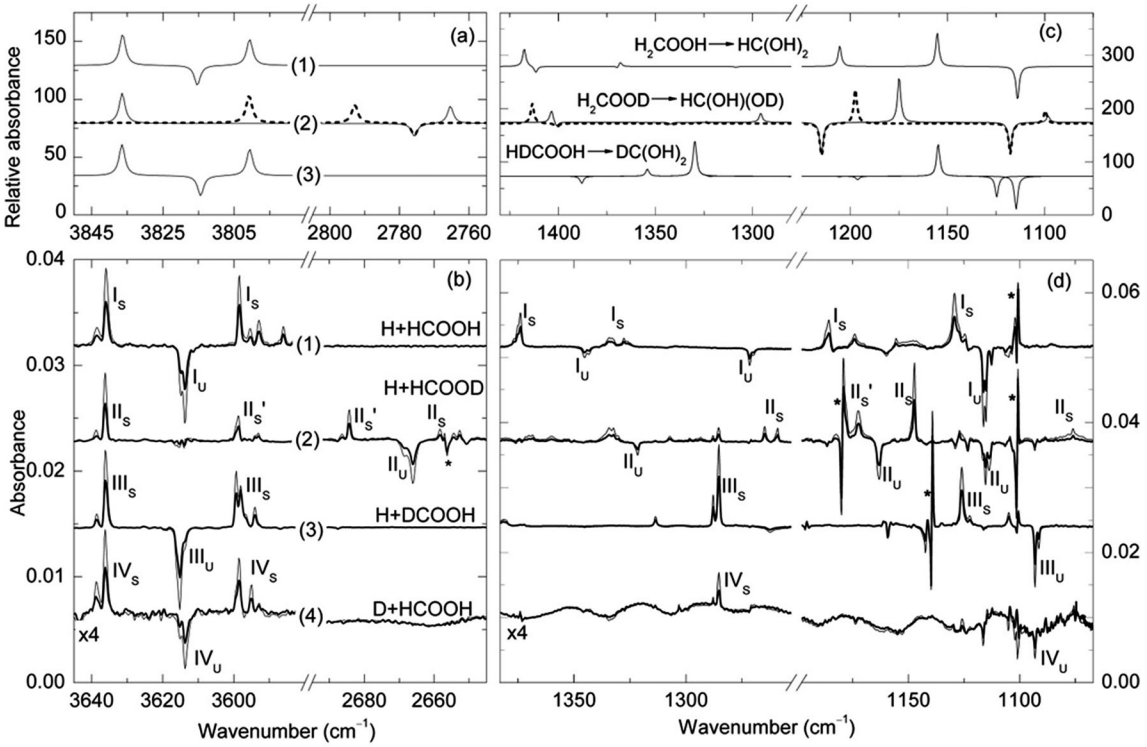

Fig. 4 (a and c) Calculated IR spectra of *trans*-H_2COOH (negative bands) and *trans–cis*-$HC(OH)_2$ (positive bands) and their deuterated analogues. The dashed line in the calculated spectrum (2) corresponds to *trans–cis*-HC(OH)(OD) with the *cis*-OD group. The splitting of the negative band in the calculated spectrum (3) of *trans*-HDCOOH is caused by different locations of the CD group. (b and d) Difference IR spectra showing the conversion processes after different reactions: (1) H + HCOOH, (2) H + HCOOD, (3) H + DCOOH, and (4) D + HCOOH. Thick and thin lines in the experimental spectra correspond to 4 and 8 hours in the dark at 4.3 K after annealing, respectively. Bands of FA are marked by asterisks. The FA/HBr (C_2D_2)/Kr matrices were first photolyzed at 193 nm and then annealed for 5 min at 31 K. The spectra were recorded at 4.3 K. Note the different absorbance scales in the left and right panels.

that of carbonic acid (9.2 kcal mol^{-1})[30] and definitely too small to stabilize the higher-energy conformer at the timescale of hours. For comparison, the *cis* form of FA converts to *trans*-FA much faster than in the present study despite the calculated stabilization barrier of 7.7 kcal mol^{-1}. The exclusion of the assignment of $\mathbf{I}_U$ to *cis–cis*-$HC(OH)_2$ is confirmed by the deuteration experiments. In particular, no OD stretching band is seen as a result of the D + HCOOH reaction (see trace 4 in Fig. 4).

After these exclusions, the most probable mechanism of the H + FA reaction is the addition of the hydrogen atom to the carbon atom, which results in the H_2COOH radical. For this radical, only one true minimum, the *trans* conformer, is found, and its total energy is higher than that of *trans–cis*-$HC(OH)_2$ by 8.10 kcal mol^{-1} (UCCSD(T)). Thus, we assign the decreasing bands to the *trans*-H_2COOH radical and the rising bands to the *trans–cis*-$HC(OH)_2$ radical. Our spectroscopic data show that the *trans*-H_2COOH radical dominates immediately after annealing (trace 1 in Fig. 2 and Fig. 3 and 5) and then it slowly converts to *trans–cis*-$HC(OH)_2$.

The amount of hydrogen atoms in the 193 nm irradiated HCOOH/HBr/Kr (1/2/1000) matrix is roughly twice as much as the amount of remaining FA molecules. It follows that the initial product of the H + FA reaction (*trans*-H_2COOH) may in principle react with a second hydrogen atom to form the closed-shell species $CH_2(OH)_2$ (methanediol). This molecule has been observed in an Ar matrix and its vibrational spectrum is different from the spectra of our species.[31] For example, the strong CO stretching band of $CH_2(OH)_2$ is not detected in the present experiments.

Now, we analyse the spectra of the reaction products (Table 2). The OH stretching region is very informative. In theory, the *trans–cis*-$HC(OH)_2$ radical has two OH stretching bands of similar intensity separated by about 33 cm^{-1} whereas the *trans*-H_2COOH radical has one intense band located between the *trans–cis*-$HC(OH)_2$ bands. These calculations are in perfect agreement with the experiment. In the H + HCOOH experiment, product $\mathbf{I}_S$ has two bands separated by 39 cm^{-1} and product $\mathbf{I}_U$ has one OH stretching band located in between. In contrast, the calculated *cis–cis*-$HC(OH)_2$ radical has the OH stretching band higher in frequency than the two bands of *trans–cis*-$HC(OH)_2$, which also supports our assignment of the initial product to *trans*-H_2COOH.

For the H + HCOOD reaction, the OH stretching region exhibits similar rising bands as in the H + HCOOH case whereas no decreasing band appears in between. This fact strongly confirms that the unstable product is H_2COOD that has no OH stretching mode but only OD. The two rising bands

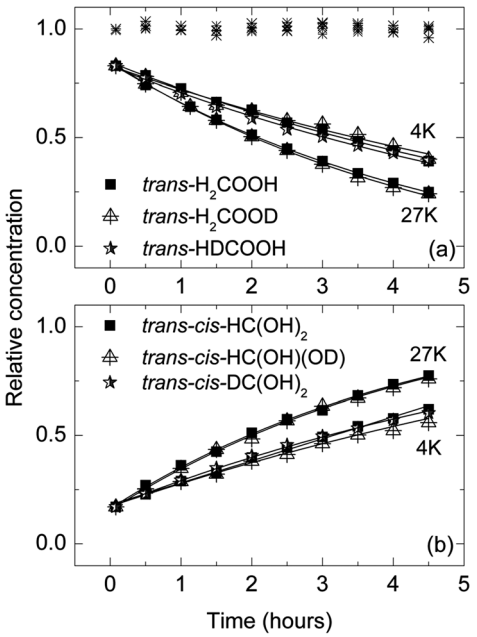

Fig. 5 Relative concentrations of the products as a function of time at different temperatures in the dark. (a) The decay of the initial products *trans*-H_2COOH (3614 cm^{-1}), *trans*-H_2COOD (2666 cm^{-1}), and *trans*-HDCOOH (3614 cm^{-1}); (b) The formation of the final products *trans–cis*-$HC(OH)_2$ (3636 cm^{-1}), *trans–cis*-HC(OH)(OD) (2684 cm^{-1}), and *trans–cis*-$DC(OH)_2$ (3636 cm^{-1}). The sum of the relative concentrations of the unstable and stable products is shown by stars in panel a.

in the OD stretching region are separated by 26 cm^{-1} and the decreasing band appears in between (trace 2 in Fig. 4b). The appearance of four (not two) rising bands is explained by the fact that the *trans–cis*-HC(OH)(OD) radical has two isotopic analogues. In this case, the bands at 3635 and 2658/2654 cm^{-1} are assigned to the species with the *cis*-OH and *trans*-OD groups. The second isotopic analogue has the *trans*-OH and *cis*-OD groups, absorbing at 3598 and 2686/2684 cm^{-1}, respectively.

For the H + DCOOH and D + HCOOH reactions, the OH stretching bands (traces 3 and 4 in Fig. 4) are similar to the H + HCOOH case for both initial and final products (trace 1). An important observation is the absence of the OD stretching bands in these two cases, which indicates that the H (not D) atom is involved in the conversion process (see also later). For the D + HCOOH reaction, the lack of the OD stretching absorption provides an additional support that the initial product is formed by the addition of a D atom to the carbon atom of FA rather than to the oxygen atom.

In the νCH and νCD regions, weak but characteristic bands are observed. For the H + HCOOH and H + HCOOD reactions, both products absorb in the CH stretching region (3100–2800 cm^{-1}) whereas the CD stretching region (2300–2000 cm^{-1}) shows no bands. For the H + DCOOH reaction, the initial product exhibits the CH and CD stretching bands at 2872.0 and 1952.0 cm^{-1}, which further confirm the addition of a hydrogen atom to the carbon atom of FA.

The spectrum in the deformation region (1400–900 cm^{-1}) also supports the proposed assignment. For the H + HCOOH reaction, the positions of the two decaying (~1116.0/1115.0 and 964.5/962.0 cm^{-1}) and three rising bands (~1326, 1186.0, and ~1129 cm^{-1}) are in good agreement with the calculations (1113.7 and 1002.2 cm^{-1} for *trans*-H_2COOH; 1368.3, 1205.3, and 1155.1 cm^{-1} for *trans–cis*-$HC(OH)_2$). For the H + HCOOD reaction, the spectrum significantly changes in qualitative agreement with the calculations. An intense band at 1288 cm^{-1} is observed for the final product for the H + DCOOH and D + HCOOH reactions but it is absent in other cases. According to the calculations, this band is characteristic of *trans–cis*-$DC(OH)_2$ (calculated frequency 1329.7 cm^{-1}). It should be admitted that some of the experimental shifts in this region are not accurately predicted. An example is the order of two rising bands and one decaying band observed in the H + HCOOD reaction at around 1150 cm^{-1}. In the experiment, the decaying band is between the two rising bands whereas the calculations predict it at a higher frequency. We connect this small discrepancy with the difficulties to describe open-shell species even at the UCCSD(T) level of theory. Very accurate calculations of vibrational spectra of open-shell species require special approaches,[32] but this exceeds the scope of the present work. Furthermore, this is not a surprise that some band intensities are not accurately predicted by the MP2 calculations.

Formation of the radicals and intramolecular hydrogen atom transfer

As shown above, new radicals *trans*-H_2COOH and *trans–cis*-$HC(OH)_2$ are formed in the H + FA reaction. Our spectroscopic data in a Kr matrix suggest that this reaction primarily produces the *trans*-H_2COOH radical by the addition of a hydrogen atom to the carbon atom of FA and this species dominates immediately after annealing. The formation of the *trans*-H_2COOH radical in the H + FA reaction is energetically favourable (by 1.91 kcal mol^{-1}) at the UCCSD(T) level of theory. This radical is higher in energy than the lowest-energy *trans–cis*-$HC(OH)_2$ species by 8.10 kcal mol^{-1} (UCCSD(T)). The situation when a reaction produces a metastable isomer is not unique to matrix-isolation studies. One example is the efficient formation of the higher-energy dimers of FA after deposition of matrices under some conditions.[33] As another example, the H + SO_2 reaction mainly leads to a higher-energy isomer HSO_2 but not to the ground-state isomer HOSO.[23]

The experimental results show that the initial product *trans*-H_2COOH converts to the *trans–cis*-$HC(OH)_2$ radical in the dark at cryogenic temperature (4.3 K). We explain this isomerization process by intramolecular hydrogen-atom tunneling from carbon to oxygen atom. This process agrees with the calculated energetics of the system showing that the *trans*-H_2COOH radical is higher in energy than the *trans–cis*-$HC(OH)_2$. The *trans*-H_2COOH stabilization barrier is high enough (21.31 kcal mol^{-1} at the UMP2 level of theory) to prevent the over-barrier process at low temperatures; however, quantum tunneling of a hydrogen atom is possible through this barrier. The tunneling mechanism is supported by the strong H/D isotope effect: (i) no OD stretching bands appear as a result of the conversion of HDCOOH and (ii) D_2COOH is practically stable. The strong H/D isotope effect has been repeatedly shown for quantum tunneling.[34,35]

The *cis–cis*-$HC(OH)_2$ radical can be formed in this tunneling process but quickly decays to the *trans–cis* conformer due to the very low stabilization barrier (0.44 kcal mol^{-1}). It has been recently reported that methylhydroxycarbene ($H_3C–C–OH$) isomerizes to acetaldehyde ($H_3C–CH{=}O$) with a lifetime *ca.* 1 hour in an Ar matrix at 11 K, and the process was explained by a facile hydrogen tunneling through a barrier of 28.0 kcal mol^{-1}.[36]

The isomerization from *trans*-H_2COOH to *trans–cis*-$HC(OH)_2$ is accelerated by vibrational excitation of νOH fundamental by the narrow-band IR light but the opposite process does not occur. This fact fully agrees with the computational energies showing a significantly higher isomerization barrier (35.73 kcal mol^{-1}) for the opposite process. It should be noted that the photon energy (3536 cm^{-1} or 10.1 kcal mol^{-1}) is smaller than the calculated stabilization barrier of *trans*-H_2COOH; however, light-induced under-barrier tunneling was demonstrated.[37] The conversion process is accelerated by broad-band IR light even for D_2COOH, which is probably contributed by an over-barrier isomerization. Furthermore, this hydrogen-atom tunneling mechanism is consistent with the acceleration of the conversion process at elevated temperatures (*ca.* 7.5 hours at 4 K and 5.0 hours at 27 K), which is typical for quantum tunneling.[34,35]

Radical isomerization *via* hydrogen atom tunneling can compete with radical decomposition. In the present case, the possible decomposition channel would lead to H_2 + COOH (or HOCO). However, no evidence of these species is provided by the experiments as mentioned above. Another remarkable fact is that the present situation is quite different from the Cl + FA reaction leading to HCl.[9] It can also be noted that the weak *trans–cis*-$HC(OH)_2$ bands are seen immediately after annealing (trace 1 in Fig. 2). This observation seemingly suggests that some amount of this species is formed directly in the H + FA reaction. However, more probably, these weak bands appear due to the isomerization during the annealing and the first measurement.

Conclusions

This work presents the first report on the reaction of atomic hydrogen with formic acid. The experiments in a Kr matrix show that this reaction proceeds *via* addition of the hydrogen atom to the carbon atom of FA to form the *trans*-H_2COOH radical as the initial product. The *trans*-H_2COOH radical isomerizes *via* intramolecular hydrogen atom tunneling to the lower-energy *trans–cis*-$HC(OH)_2$ radical, which is the simplest geminal diol radical. These two radicals are directly observed for the first time and characterized by using IR spectroscopy and *ab initio* calculations at the UMP2 and UCCST(T) levels of theory. The assignment of the products and the hydrogen atom tunneling mechanism of the isomerization are confirmed by experiments with deuterated species.

The simplest geminal diol radical *trans–cis*-$HC(OH)_2$ obtained and identified in the present work is presumably very reactive, and further reaction channels are of particular interest. For instance, these species may constitute new channels for the initiation and propagation of more complex organic species in the interstellar clouds.[38] To our knowledge, the new reactions and species observed in the present work have not been considered in these interstellar processes. Another natural extension of this work is the study of reactions between atomic hydrogen and more complex molecules such as amino and fatty acids.

Acknowledgements

The work was supported by the Academy of Finland (Grant code 1139425) and the National Center for Research and Development of Poland (grant ERA-CHEMISTRY-2009/01/2010). The Wroclaw Center for Networking and Supercomputing and the CSC–IT Center for Science in Espoo are acknowledged for allocated computational resources.

Notes and references

1 W. E. Jones, S. D. Macknight and L. Teng, *Chem. Rev.*, 1973, **73**, 407–440.
2 J. Villà, A. González-Lafont, J. M. Lluch and D. G. Truhlar, *J. Am. Chem. Soc.*, 1998, **120**, 5559–5567.
3 J. P. Camden, H. A. Bechtel, D. J. Ankeny Brown, M. R. Martin, R. N. Zare, W. Hu, G. Lendvay, D. Troya and G. C. Schatz, *J. Am. Chem. Soc.*, 2005, **127**, 11898–11899.
4 R. B. Bohn, G. D. Brabson and L. Andrews, *J. Phys. Chem.*, 1992, **96**, 1582–1589.
5 M. Yamada and A. Amano, *Ind. Eng. Chem. Res.*, 1992, **31**, 8–13.
6 K. Hiraoka, A. Yamashita, T. Miyagoshi, N. Oohashi, Y. Kihara and K. Yamamoto, *Astrophys. J.*, 1998, **508**, 423–430.
7 S. E. Bisschop, G. W. Fuchs, E. F. van Dishoeck and H. Linnartz, *Astron. Astrophys.*, 2007, **474**, 1061–1071.
8 W. M. Garrison, W. Bennett, S. Cole, H. R. Haymond and B. M. Weeks, *J. Am. Chem. Soc.*, 1955, **77**, 2720–2727.
9 Q. Li, M. C. Osborne and I. W. M. Smith, *Int. J. Chem. Kinet.*, 2000, **32**, 85–91.
10 A. Miyoshi, H. Matsui and N. Washida, *J. Chem. Phys.*, 1994, **100**, 3532–3539.
11 G. S. Tyndall, T. J. Wallington and A. R. Potts, *Chem. Phys. Lett.*, 1991, **186**, 149–153.
12 M. Pettersson, J. Lundell, L. Khriachtchev and M. Räsänen, *J. Am. Chem. Soc.*, 1997, **119**, 11715–11716.
13 E. M. S. Maçôas, L. Khriachtchev, M. Pettersson, R. Fausto and M. Räsänen, *J. Am. Chem. Soc.*, 2003, **125**, 16188–16189.
14 E. M. S. Maçôas, L. Khriachtchev, M. Pettersson, R. Fausto and M. Räsänen, *J. Phys. Chem. A*, 2005, **109**, 3617–3624.
15 S. Amiri, H. P. Reisenauer and P. R. Schreiner, *J. Am. Chem. Soc.*, 2010, **132**, 15902–15904.
16 L. Khriachtchev, A. Domanskaya, K. Marushkevich, M. Räsänen, B. Grigorenko, A. Ermilov, N. Andrijchenko and A. Nemukhin, *J. Phys. Chem. A*, 2009, **113**, 8143–8146.
17 C. L. Hawkins and M. J. Davies, *Biochim. Biophys. Acta*, 2001, **1504**, 196–219.

18 F. Turecek and E. A. Syrstad, *J. Am. Chem. Soc.*, 2003, **125**, 3353–3369.
19 H. Tanskanen, L. Khriachtchev, M. Räsänen, V. I. Feldman, F. F. Sukhov, A. Yu. Orlov and D. A. Tyurin, *J. Chem. Phys.*, 2005, **123**, 064318.
20 M. Pettersson, J. Lundell, L. Khriachtchev and M. Räsänen, *J. Chem. Phys.*, 1998, **109**, 618.
21 M. Pettersson, L. Khriachtchev, S. Jolkkonen and M. Räsänen, *J. Phys. Chem. A*, 1999, **103**, 9154–9162.
22 L. Khriachtchev, S. Tapio, A. Domanskaya, M. Räsänen, K. Isokoski and J. Lundell, *J. Chem. Phys.*, 2011, **134**, 124307.
23 E. Isoniemi, L. Khriachtchev, J. Lundell and M. Räsänen, *Phys. Chem. Chem. Phys.*, 2002, **4**, 1549–1554.
24 J. Lundell and M. Räsänen, *J. Phys. Chem.*, 1995, **99**, 14301–14308.
25 A. Domanskaya, K. Marushkevich, L. Khriachtchev and M. Räsänen, *J. Chem. Phys.*, 2009, **130**, 154509.
26 L. Khriachtchev, M. Saarelainen, M. Pettersson and M. Räsänen, *J. Chem. Phys.*, 2003, **118**, 6403–6410.
27 L. Khriachtchev, H. Tanskanen, A. Cohen, R. B. Gerber, J. Lundell, M. Pettersson, H. Kiljunen and M. Räsänen, *J. Am. Chem. Soc.*, 2003, **125**, 6876–6877.
28 Q. Cao, S. Berski, M. Räsänen, Z. Latajka and L. Khriachtchev, *J. Phys. Chem. A*, 2013, **117**, 4385–4393.
29 J. Bernard, M. Seidl, I. Kohl, K. R. Liedl, E. Mayer, Ó. Gálvez, H. Grothe and T. Loerting, *Angew. Chem., Int. Ed.*, 2011, **50**, 1939–1943.
30 C. A. Wight and A. I. Boldyrev, *J. Phys. Chem.*, 1995, **99**, 12125–12130.
31 C. Lugez, A. Schriver, R. Levant and L. Schriver-Mazzuoli, *Chem. Phys.*, 1994, **181**, 129–146.
32 R. Tarroni, L. Khriachtchev, A. Domanskaya, M. Räsänen, E. Misochko and A. Akimov, *Chem. Phys. Lett.*, 2010, **493**, 220–224.
33 K. Marushkevich, L. Khriachtchev, M. Räsänen, M. Melavuori and J. Lundell, *J. Phys. Chem. A*, 2012, **116**, 2101–2108.
34 V. I. Goldanskii, L. I. Trakhtenberg and V. N. Fleurov, *Tunneling Phenomena in Chemical Physics*, Gordon and Breach Science, New York, 1989.
35 L. Khriachtchev, *J. Mol. Struct.*, 2008, **880**, 14–22.
36 P. R. Schreiner, H. P. Reisenauer, D. Ley, D. Gerbig, C.-H. Wu and W. D. Allen, *Science*, 2011, **332**, 1300–1303.
37 M. Pettersson, E. M. S. Maçôas, L. Khriachtchev, R. Fausto and M. Räsänen, *J. Am. Chem. Soc.*, 2003, **125**, 4058–4059.
38 A. G. G. M. Tielens and L. J. Allamandola, in *Physics and Chemistry at Low Temperatures*, ed. L. Khriachtchev, Pan Stanford Publishing, Singapore, 2011, pp. 341–380.
39 K. Marushkevich, M. Siltanen, M. Räsänen, L. Halonen and L. Khriachtchev, *J. Phys. Chem. Lett.*, 2011, **2**, 695–699.